Interventional cardiovascular magnetic resonance imaging

Venkatesh K. Raman and **Robert J. Lederman**
From the Cardiovascular Branch (VKR and RJL), Division of Intramural Research, National Heart Lung and Blood Institute, National Institutes of Health, Bethesda, MD, USA and the Washington DC Veterans Affairs Medical Center (VKR), Washington, DC, USA.

Abstract

Magnetic resonance imaging (MRI) provides structural and functional cardiovascular information with excellent soft tissue contrast. Real-time MRI can guide transcatheter cardiovascular interventions in large animal models, and may prove superior to x-ray and adjunct modalities for peripheral vascular, structural heart and cardiac electrophysiology applications. We describe technical considerations, pre-clinical work and early clinical studies in this emerging field.

Introduction

Since Dotter and Judkins first introduced transluminal angioplasty over 40 years ago, X-ray-guided catheter-based cardiovascular treatments have become widely adopted. Increasingly complex procedures have driven development of adjunctive imaging such as intravascular ultrasound.

Though versatile, X-ray fluoroscopy suffers from a lack of specific soft tissue contrast and only reveals blood vessels when filled with contrast agents. The ionizing radiation risks late cancer, especially in younger patients undergoing multiple procedures (Modan et al. 2000).

Commercial magnetic resonance imaging (MRI) systems can now examine the heart in real-time. Images can be based on a range of mechanisms, such as water or fat content, macromolecule interaction, blood velocity, or accumulation of exogenous contrast.

This paper describes the prospects and challenges for MRI to guide catheter-based cardiovascular treatments. We review technical requirements for interventional cardiovascular magnetic resonance imaging (iCMR) as well as preclinical and clinical experience to date.

Technical Considerations

Imaging environment

Catheter-based cardiovascular intervention requires real-time imaging, defined as rapid data acquisition with nearly instantaneous image reconstruction and image display. Most iCMR investigators use 1.5 Tesla systems, balancing increased signal-to-noise (SNR) at higher field strengths against higher entropic signal decay. Rapid MRI, even at 1.5T, approaches

physiologic limits of heating from radiofrequency energy deposition and nerve stimulation from oscillating magnetic fields, which are exacerbated at higher field strengths.

Contemporary hardware enables fast pulse sequences, such as steady-state free precession (SSFP) (Oppelt 1986). SSFP is particularly suited to iCMR because SNR is high, and blood appears bright. Enhancements include echo sharing, which recycles image data across multiple frames and increases perceived imaging speed although temporal resolution remains unchanged. Undersampling and interpolation exploit symmetries within frequency data (k-space) to reduce acquisition time. Parallel imaging exploits the added "perspective" of different surface receiver coils to increase speed (Pruessmann et al. 1999). Combined, such techniques can provide more than 10 useful frames per second, sufficient to guide many procedures.

Interactive graphical user interfaces allow operators to adjust imaging planes, imaging speed, field-of-view and contrast characteristics "on the fly" during procedures.(Guttman et al. 2002). These often are implemented on external workstations to provide additional computational horsepower. Single or multiple imaging planes, adjusted interactively or automatically, can target specific anatomy or track interventional devices. Magnetization pre-pulses can brighten or darken specific tissues, for example to enhance accumulation of gadolinium contrast or to hide fatty tissue.

MRI creates safety challenges. Ferromagnetic components can render ordinary objects into deadly projectiles within the strong magnetic field. Long conductive wires, such as guidewires and braided catheters, can cause inductive heating during radiofrequency excitation (see below). Electrocardiographic signals are distorted by bulk blood flow through the aorta (magnetohydrodynamic effect), which coincides with the ST-segment used to monitor myocardial injury. Standard emergency equipment such as defibrillators must be operated outside the strong magnetic field, because the high currents generate strong mechanical displacement forces. For this reason, and because X-ray fluoroscopy may become necessary for emergency bail-out procedures, iCMR laboratories should have a dependable patient transport system and evacuation strategy. Reverberations from rapid gradient oscillation cause intolerable acoustic noise during scanning. This requires sound suppression equipment for staff and patient communication.

Interventional devices

Contemporary interventional devices balance miniaturization, flexibility, trackability, and torque control. Most include steel braid for mechanical stiffness and X-ray conspicuity. Ferrous components, however, destroy MR images. Removing the ferrous components leaves the devices invisible under MRI. Replacing them with MRI-compatible metals (such as nitinol or platinum) leaves the devices susceptible to inductive heating (Figure 1). Indeed, developing safe yet conspicuous catheter devices remains the greatest remaining challenge to iCMR. There are two general approaches to this problem.

Devices can be visualized "passively" based on their intrinsic material characteristics. One approach is to embed small quantities of superparamagnetic materials, such as dysprosium or iron oxide, into the catheters to create signal voids (black spots). Superparamagnetic markers create MRI "blooming" artifacts that are much larger than the markers themselves.

Imaging signal voids has limitations. The "blooming" effect may obscure target anatomy and important device features such as stent edges. Black spots are nonspecific, because many phenomena can result in MR signal loss, including tissue borders and high velocity blood jets.

Moreover, the signal voids used to track devices can be obscured within large voxels through combination with tissue elements of higher signal intensity. This volume averaging causes catheters to appear "lost" because the signal void is averaged or blended out.

Other passive approaches include filling balloon catheters with CO_2 (dark signal) (Razavi et al. 2003) or gadolinium (bright signal) (Yang et al. 2000). One team has reported limited success coating catheters with contrast agents such as gadolinium (Unal et al. 1998). Despite the limitations of passive devices, most early iCMR experiences use them because of their relative simplicity, safety, and wide availability.

"Active" catheters incorporate receiver coils that detect excited spins nearby. The resulting antenna-catheters are connected to the MRI hardware to help track or visualize them. Several antenna designs have been evaluated, including loop, dipole or loopless, and solenoid devices (McKinnon et al. 1996).

Active catheters can be used in at least two modes. In "tracking" mode, marker coils on the catheter are tracked by using non-imaging scan sequences. Coil locations are depicted with computer-synthesized markers superimposed on images. Early active catheters were localized precisely by tracking such microcoils (Dumoulin et al. 1993; Leung et al. 1995). An alternative strategy is to "profile" or display longer lengths of active catheters which incorporate different antenna designs (Figure 1**C**). Signals from the profile active catheter and surface MRI receiver coils are combined to create images that usually depict the catheter alongside surrounding tissue. One clinically-tested intravascular MR device is a loopless design 0.030" nitinol guidewire (Ocali et al. 1997).

Active and other conductive catheter devices also risk intravascular thermal injury because of radiofrequency-induced currents (Yeung et al. 2002). Several strategies can control this problem, including detuning and decoupling the circuit (Ocali et al. 1997; Ladd et al. 2000), incorporating transformers into the transmission lines (Eggers et al. 2003), using fiberoptic transmission lines (Wong, Zhang et al. 2000), using inductively coupled "wireless" resonators that obviate transmission lines (Quick et al. 2002), or using multispectral MRI to track catheters incorporating hyperpolarized ^{13}C or ^{19}F (Svensson et al. 2003), (Kozerke et al. 2004).

Interventional cardiovascular MRI – applications

Pre-clinical experience

Early feasibility studies for iCMR generally targeted large peripheral vessels not subject to significant cardiac and respiratory motion. Coronary angiography, angioplasty and stent deployment in normal swine have been described (Spuentrup et al. 2002; Serfaty et al. 2003), primarily highlighting visualization and tracking techniques or advances in rapid imaging. Spatial resolution probably will remain inadequate to guide meaningful clinical coronary artery interventional procedures. Carotid, renal and ilio-femoral arteries have been successfully accessed for angiography and angioplasty solely under MRI (Omary et al. 2000; Feng et al. 2005a; Feng et al. 2005b; Elgort et al. 2006), although such treatments are routinely successful under X-ray alone. A more compelling application is MR-guided treatment of aortic disease. Eggebrecht and colleagues visualized aortic dissection, not generally conspicuous under X-ray, and demonstrated complete obliteration of the false lumen in a porcine model(Eggebrecht et al. 2006) (Figure 2).

X-ray visualizes vascular spaces only when they are at least partially patent and when blood is replaced by contrast agents. Totally occluded arteries are not seen by x-ray, but can be visualized under MRI. Recanalization of chronic total arterial occlusion (CTO) represents one of the most challenging interventional procedures. Guidewire traversal through occluded

segments risks catastrophic perforation. Recent work offers hope that MRI may improve procedural safety and success. Using a custom active catheter and wire, Raval and colleagues recanalized occluded carotid arteries in swine even after X-ray failure (Raval et al. 2006). Multislice real-time MRI depicted the occluded vessel and guided safe passage of the relatively stiff guidewire (Figure 3).

This CTO experience suggests that applications need not respect vascular boundaries that confine contemporary catheter-based interventional procedures. The first such catheter-based extra-anatomic bypass is the transjugular intrahepatic portosystemic shunt (TIPS) procedure conducted to relieve portal hypertension. Intrahepatic puncture of the portal vein under MR-guidance was first described in 1997 (Wildermuth et al. 1997). More recently, Arepally and colleagues used MRI to create a selective mesocaval (vena cava to mesenteric or splenic vein) communication, previously possible only with more risky open surgery (Arepally et al. 2006) (Figure 4).

Congenital and structural heart disease treatments may benefit from the capabilities of MRI. Real-time imaging in multiple, arbitrary, and non-orthogonal planes may enhance visual reconstruction of complex anatomical relationships and guide interventions. Rickers et al closed iatrogenic atrial septal defects in swine using a commercial nitinol occluder (Rickers et al. 2003). Right atrial and ventricular volumes were shown to decrease during post-procedural scanning, demonstrating the utility and convenience of using a single modality.

Cells, genes or drugs may be targeted and deposited in high local concentrations, conceivably attenuating systemic toxicity and complementing molecular homing mechanisms. Dick et al reported the use of rtMRI for cell delivery by customized injection catheter to infarct border in a swine model (Dick et al. 2003) (Figure 5). This study highlighted real-time infarct imaging, anatomically targeted endomyocardial injection, and verification of delivery using an intracellular MRI contrast agent.

Cardiac electrophysiology treatments already import multi-modality data for complex mapping and ablation. Electro-anatomic representations and CT/MR fusion are now routinely part of complex mapping and ablation procedures, overlaid on X-ray fluoroscopic images. These techniques have intrinsic limitations as "roadmaps". Because MRI depicts atrial and pulmonary vein anatomy well, iCMR may prove useful to treating rhythm disorders, including immediate visualization of the extent and continuity of tissue ablation (Dickfeld et al. 2007). Several groups have customized catheters to permit endocardial electrogram acquisition and shown preliminary feasibility for electro-anatomic mapping under MR guidance (Susil et al. 2002).

Clinical Translation

In seminal work, Razavi et al report diagnostic catheterization in patients with congenital disease using a hybrid XMR (x-ray-MRI) system (Razavi et al. 2003) (Figure 6). Investigators in Regensburg have conducted clinical iCMR femoropopliteal angioplasty using passive commercial devices solely under MRI guidance (Manke et al. 2001; Paetzel et al. 2004). Kee and colleagues, working on a novel integrated X-ray/MRI system, successfully performed TIPS procedures in 13 out of 14 patients with fewer attempted punctures and less fluoroscopy time (Kee et al. 2005). A team of pediatric cardiologists in Berlin recently reported their initial experience with MR-guided angioplasty for aortic coarctation (Krueger et al. 2006). Other groups are working toward clinical investigation of iCMR for the treatment of peripheral artery, structural heart, and cardiac rhythm disorders, using both passive and active catheter devices.

Conclusion

With *in situ* anatomic depiction that surpasses what is available in open surgery, MRI promises to improve and expand the breadth of minimally-invasive non-surgical therapies. The principal barrier to further development is the limited availability of safe and conspicuous clinical-grade catheter devices. Now that several academic centers are beginning to focus on development of investigational clinical devices, we can expect a flurry of new developments to enhance interventional treatment options for patients.

References

Arepally A, Karmarkar PV, Qian D, Barnett B, Atalar E. Evaluation of MR/fluoroscopy-guided portosystemic shunt creation in a swine model. J Vasc Interv Radiol 2006;17:1165–1173. [PubMed: 16868170]

Dick AJ, Guttman MA, Raman VK, Peters DC, Pessanha BSS, Hill JM, et al. Magnetic resonance fluoroscopy allows targeted delivery of mesenchymal stem cells to infarct borders in swine. Circulation 2003;108:2899–2904. [PubMed: 14656911]

Dickfeld T, Kato R, Zviman M, Nazarian S, Dong J, Ashikaga H, et al. Characterization of acute and subacute radiofrequency ablation lesions with nonenhanced magnetic resonance imaging. Heart Rhythm 2007;4:208–214. [PubMed: 17275759]

Dumoulin CL, Souza SP, Darrow RD. Real-time position monitoring of invasive devices using magnetic resonance. Magn Reson Med 1993;29:411–415. [PubMed: 8450752]

Eggebrecht H, Kuhl H, Kaiser GM, Aker S, Zenge MO, Stock F, et al. Feasibility of real-time magnetic resonance-guided stent-graft placement in a swine model of descending aortic dissection. Eur Heart J 2006;27:613–620. [PubMed: 16431874]

Eggers H, Weiss S, Boernert P, Boesiger P. Image-based tracking of optically detunable parallel resonant circuits. Magn Reson Med 2003;49:1163–1174. [PubMed: 12768595]

Elgort DR, Hillenbrand CM, Zhang S, Wong EY, Rafie S, Lewin JS, et al. Image-guided and -monitored renal artery stenting using only MRI. J Magn Reson Imaging 2006;23:619–627. [PubMed: 16555228]

Feng L, Dumoulin CL, Dashnaw S, Darrow RD, Delapaz RL, Bishop PL, et al. Feasibility of stent placement in carotid arteries with real-time MR imaging guidance in pigs. Radiology 2005a;234:558–562. [PubMed: 15591432]

Feng L, Dumoulin CL, Dashnaw S, Darrow RD, Guhde R, Delapaz RL, et al. Transfemoral catheterization of carotid arteries with real-time MR imaging guidance in pigs. Radiology 2005b;234:551–557. [PubMed: 15591433]

Guttman MA, Lederman RJ, Sorger JM, McVeigh ER. Real-time volume rendered MRI for interventional guidance. J Cardiovasc Magn Reson 2002;4:431–442. [PubMed: 12549231]

Hegde S, Miquel ME, Boubertakh R, Gilderdale D, Muthurangu V, Keevil SF, et al. Interactive MR imaging and tracking of catheters with multiple tuned fiducial markers. J Vasc Interv Radiol 2006;17:1175–1179. [PubMed: 16868171]

Kee ST, Ganguly A, Daniel BL, Wen Z, Butts K, Shimikawa A, et al. MR-guided transjugular intrahepatic portosystemic shunt creation with use of a hybrid radiography/MR system. J Vasc Interv Radiol 2005;16:227–234. [PubMed: 15713923]

Kozerke S, Hegde S, Schaeffter T, Lamerichs R, Razavi R, Hill DL. Catheter tracking and visualization using 19F nuclear magnetic resonance. Magn Reson Med 2004;52:693–697. [PubMed: 15334594]

Krueger JJ, Ewert P, Yilmaz S, Gelertner D, Peters B, Pietzner K, et al. Magnetic resonance imaging-guided balloon angioplasty of coarctation of the aorta: a pilot study. Circulation 2006;113:1093–1100. [PubMed: 16490822]

Ladd ME, Quick HH. Reduction of resonant RF heating in intravascular catheters using coaxial chokes. Magn Reson Med 2000;43:615–619. [PubMed: 10748440]

Leung DA, Debatin JF, Wildermuth S, McKinnon GC, Holtz D, Dumoulin CL, et al. Intravascular MR tracking catheter: preliminary experimental evaluation. AJR Am J Roentgenol 1995;164:1265–1270. [PubMed: 7717244]

Manke C, Nitz WR, Djavidani B, Strotzer M, Lenhart M, Volk M, et al. MR imaging-guided stent placement in iliac arterial stenoses: a feasibility study. Radiology 2001;219:527–534. [PubMed: 11323483]

McKinnon GC, Debatin JF, Leung DA, Wildermuth S, Holtz DJ, von Schulthess GK. Towards active guidewire visualization in interventional magnetic resonance imaging. Magma 1996;4:13–18. [PubMed: 8773997]

Modan B, Keinan L, Blumstein T, Sadetzki S. Cancer following cardiac catheterization in childhood. Int J Epidemiol 2000;29:424–428. [PubMed: 10869313]

Ocali O, Atalar E. Intravascular magnetic resonance imaging using a loopless catheter antenna. Magn Reson Med 1997;37:112–118. [PubMed: 8978639]

Omary RA, Frayne R, Unal O, Warner T, Korosec FR, Mistretta CA, et al. MR-guided angioplasty of renal artery stenosis in a pig model: a feasibility study. J Vasc Interv Radiol 2000;11:373–381. [PubMed: 10735435]

Oppelt A. FISP - a new fast MRI sequence. Electromedica 1986;54:15–18.

Paetzel C, Zorger N, Bachthaler M, Volk M, Seitz J, Herold T, et al. Feasibility of MR-guided angioplasty of femoral artery stenoses using real-time imaging and intraarterial contrast-enhanced MR angiography. Rofo 2004;176:1232–1236. [PubMed: 15346256]

Pruessmann KP, Weiger M, Scheiddeger MB, Boesiger P. SENSE: sensitivity encoding for fast MRI. Magn Reson Med 1999;42:952–962. [PubMed: 10542355]

Quick HH, Kuehl H, Kaiser G, Bosk S, Debatin JF, Ladd ME. Inductively coupled stent antennas in MRI. Magn Reson Med 2002;48:781–790. [PubMed: 12417992]

Raval AN, Karmarkar PV, Guttman MA, Ozturk C, Sampath S, DeSilva R, et al. Real-time magnetic resonance imaging-guided endovascular recanalization of chronic total arterial occlusion in a swine model. Circulation 2006;113(8):1101–1107. [PubMed: 16490819]

Razavi R, Hill DL, Keevil SF, Miquel E, Muthurangu V, Hegde S, et al. Cardiac catheterisation guided by MRI in children and adults with congenital heart disease. Lancet 2003;362:1877–1882. [PubMed: 14667742]

Rickers C, Jerosch-Herold M, Hu X, Murthy N, Wang X, Kong H, et al. Magnetic resonance image-guided transcatheter closure of atrial septal defects. Circulation 2003;107:132–138. [PubMed: 12515755]

Serfaty JM, Yang X, Foo TK, Kumar A, Derbyshire A, Atalar E. MRI-guided coronary catheterization and PTCA: A feasibility study on a dog model. Magn Reson Med 2003;49:258–263. [PubMed: 12541245]

Spuentrup E, Ruebben A, Schaeffter T, Manning WJ, Gunther RW, Buecker A. Magnetic resonance--guided coronary artery stent placement in a swine model. Circulation 2002;105:874–879. [PubMed: 11854130]

Susil RC, Yeung CJ, Halperin HR, Lardo AC, Atalar E. Multifunctional interventional devices for MRI: a combined electrophysiology/MRI catheter. Magn Reson Med 2002;47:594–600. [PubMed: 11870847]

Svensson J, Mansson S, Johansson E, Petersson JS, Olsson LE. Hyperpolarized 13C MR angiography using trueFISP. Magn Reson Med 2003;50:256–262. [PubMed: 12876701]

Unal O, Korosec FR, Frayne R, Strother CM, Mistretta CA. A rapid 2D time-resolved variable-rate k-space sampling MR technique for passive catheter tracking during endovascular procedures. Magn Reson Med 1998;40:356–362. [PubMed: 9727937]

Wildermuth S, Debatin JF, Leung DA, Dumoulin CL, Darrow RD, Ulschmid G, et al. MR imaging-guided intravascular procedures: initial demonstration in a pig model. Radiology 1997;202:578–583. [PubMed: 9015094]

Yang X, Atalar E. Intravascular MR imaging-guided balloon angioplasty with an MR imaging guide wire: feasibility study in rabbits. Radiology 2000;217:501–506. [PubMed: 11058652]

Yeung CJ, Susil RC, Atalar E. RF safety of wires in interventional MRI: using a safety index. Magn Reson Med 2002;47:187–193. [PubMed: 11754458]
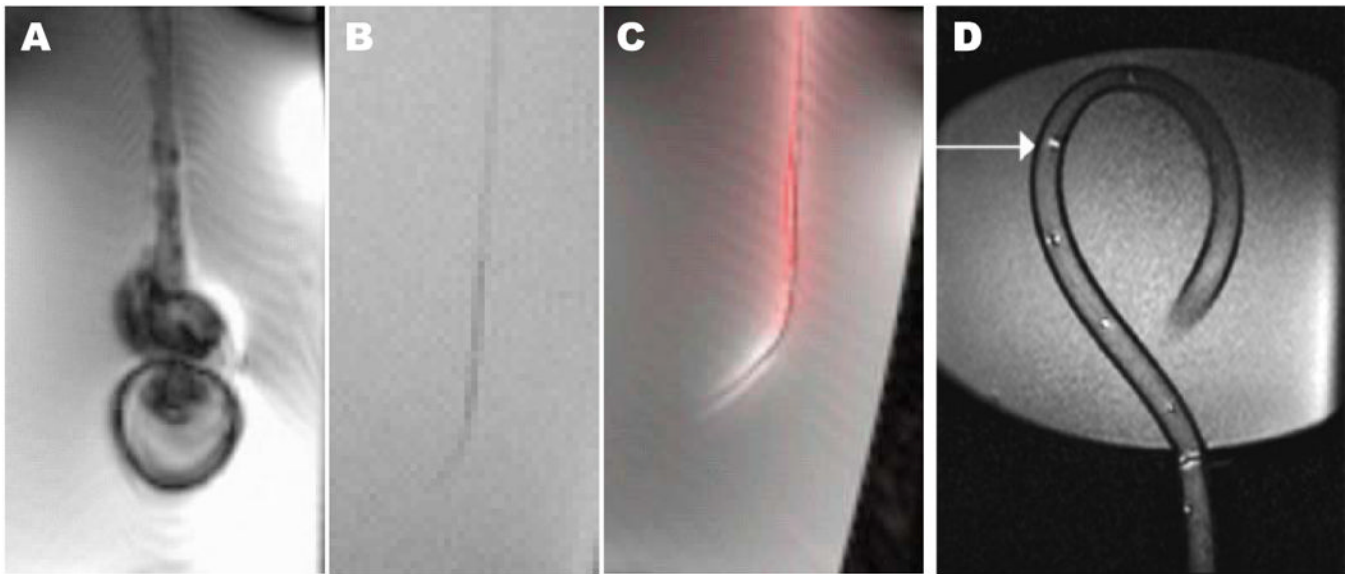
Figure 1.
Comparison of catheter visibility *in vitro* using steady-state free precession MRI. (A) A conventional steel-braided catheter disturbs the local magnetic field and distorts the image. (B) Removing the steel braid renders the catheter indistinct under MRI because it has no excitable spins to produce signal. (C) The same catheter, converted into an "active" antenna, detects excited surrounding spins and now is highly visible. Conspicuity is enhanced by post-processing techniques including gain adjustment and color highlighting. (D) A different active catheter device (Hegde et al, 2006) using multiple tuned microcoils that can be used in profiling mode or tracking mode.
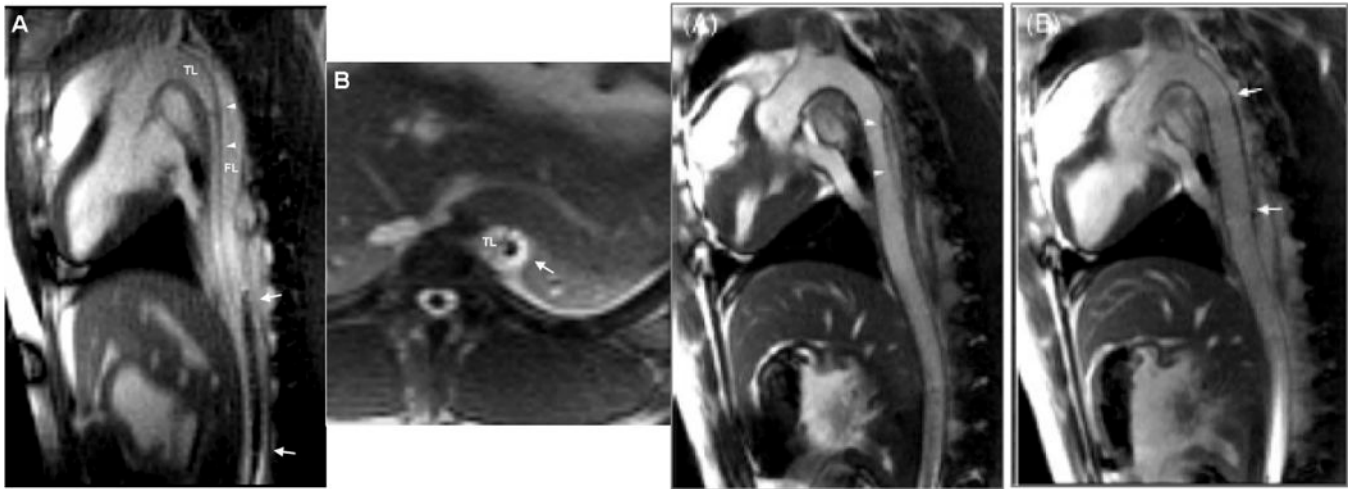
Figure 2.
MR-guided endograft treatment of aortic dissection. (A & B) Real-time sagittal and axial slices of the thoracic and abdominal aorta show dissection flap (arrowheads) separating the true lumen (TL) and false lumen (FL). The endograft delivery system is visualized passively as it is advanced through the aorta (arrows). In these views, the device has entered the false lumen and thereafter is redirected. (C) Following endograft deployment, the false lumen is obliterated. Adapted from Eggebrecht et al, 2006.
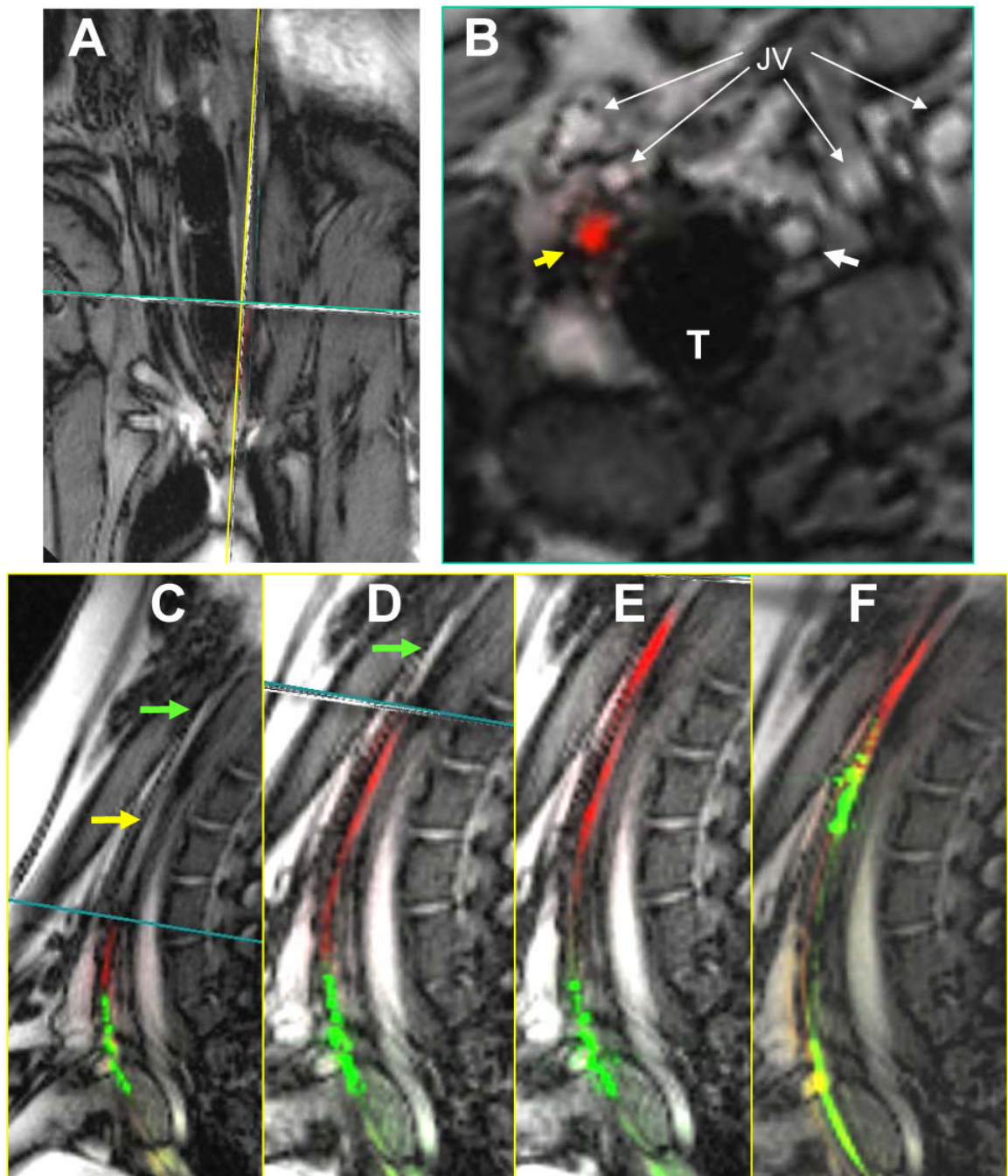
Figure 3.
Recanalization of chronic total occlusion using an active catheter and active guidewire. (A) Real-time, multiplanar MRI of the occlusion. (B) Transverse image shows the guidewire (red) traversing the occlusion (yellow arrow). (C–F) A sequence showing guidewire recanalization and catheter advancement. (C) The guidewire (red) engages the segment of interest, (D) traverses the occlusion, (E) and enters the patent distal carotid artery. (F) The catheter (green) is then advanced over the wire and across the occlusion. From Raval et al, 2006.
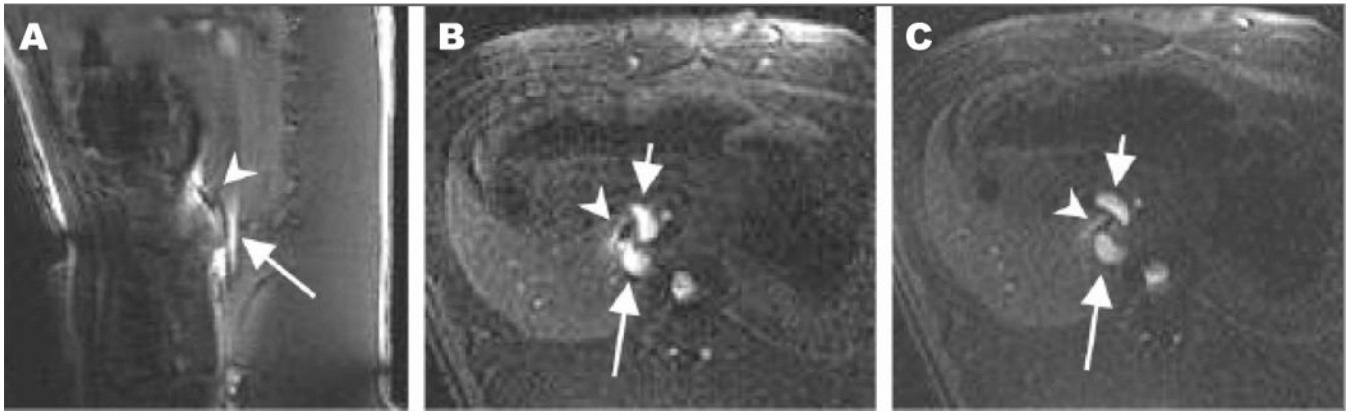
Figure 4.
Real-time puncture of superior mesenteric vein (SMV) from IVC. (A Sagittal image of needle oriented towards the SMV. Arrowhead = tip of needle, arrow = IVC. (B) The needle is seen to enter the SMV posterior wall. Adapted from Arepally et al, 2006.
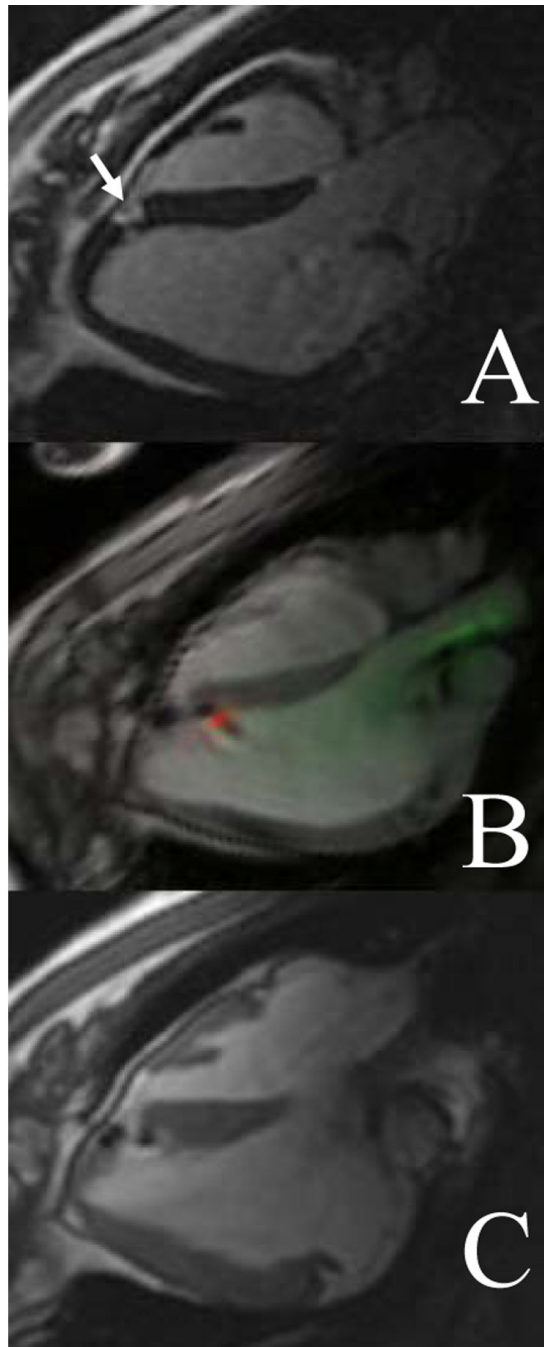
Figure 5.
Precise targeting of small infarct for MR-guided endomyocardial cell delivery. (A) Delayed gadolinium enhancement shows a small infarct (arrow) measuring approximately 1 cm^2. (B) Real-time imaging shows an active endomyocardial injection catheter (green) and needle (red) delivering cells labeled with iron oxide. (C) The cells (dark spots) are delivered to the infarct borders. From Dick et al, 2003.
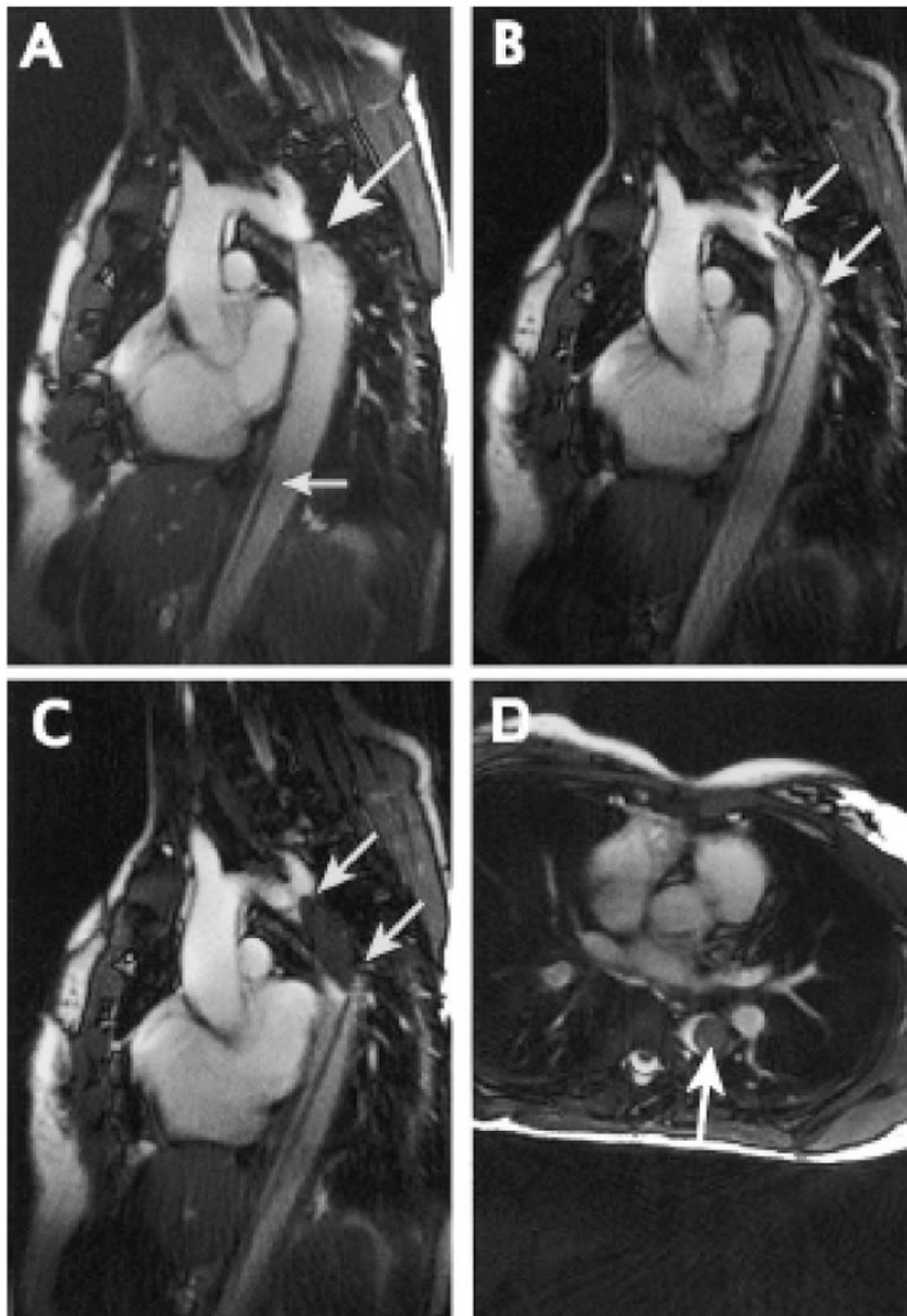
Figure 6.
MR-guided treatment of clinical aortic coarctation. (A) Real-time MRI shows aortic coarctation (large arrow). (B) Verification of catheter position across the stenosis. (C and D) Axial and sagittal views of the inflated balloon (arrows) filled with iron-oxide contrast (dark).